Bioprocess Engineering 9 (1993) 61–75

Bioprocess Engineering

Oxygenation of cell cultures

H.-J. Henzler and **D. J. Kauling,** Wuppertal, Germany

Abstract. Submersed cultures are increasingly being used for fermentation with animal cells. Reactor design is particularly important in these operations, because of the sensitivity of the cells to shear. In addition to the usual aeration methods, open-pore membranes or pure diffusion membranes are used for oxygenation in order to avoid gas bubbles. The various oxygenation methods are described in the present article [1]. Design principles for surface aeration, bubble columns, loop reactors, and stirred tanks, as well as oxygenation with Accurel or silicone membranes, are presented and discussed specifically for the low oxygen inputs desired in cell cultures. The scale laws are formulated, and special reference is made to problems of scale up. The various oxygenation methods are finally compared on the basis of the design principles presented, with particular attention to mechanical stress on the cells and to the laws of scale translation.

List of symbols

A	Interfacial area
a	= A/V, Specific interfacial area
c^*	Saturation concentration
c	Gas concentration in the liquid phase
d	Impeller diameter
d_2	Outside diameter of tubular membrane
d_1	Inside diameter of tubular membrane
d'	Diameter under stretched conditions
d_p	Particle diameter
d_L	Diameter of sparger holes
D	Reactor diameter
D_L	Draught tube diameter
$\mathbb{D}$	Gas/liquid diffusion coefficient
e	Eccentricity
Fr	Froude number
G	Mass flow
g	Acceleration due to gravity
h	Height of impeller blade
H	Filling height
Hy	Henry constant for the liquid phase
Hy_s	Henry constant of the membrane material
k	Overall mass transfer coefficient
k_L	Gas-liquid interface mass transfer coefficient
L	Length of the tubular membrane
L'	Length of the streched turbulare membrane
n	Impeller speed
Ne	$P/\rho\ n^3d^5$, Newton number
p_{O_2}	O_2-partial pressure in the membrane
$(p_{O_2})_R$	O_2-partial pressure in the reactor
P	Impeller power
q	Gas throughput
r	Cell specific respiration rate
Re	Reynolds number
Sc	$\nu/\mathbb{D}$, Schmidt number
Sh	$k_L d_2/\mathbb{D}$, Sherwood number
u	Liquid velocity
$\sqrt{\overline{u'^2}}$	Root mean square velocity of turbulent fluctuations
	Superficial gas velocity
V	Filled reactor volume
V_s	Sparged volume
X	Cell concentration
ε	Energy dissipation
η	Dynamic viscosity
ϑ	Temperature
ν	Kinematic viscosity
ρ	Density of the liquid
σ	Surface tension
τ	Shear stress

1 Oxygen requirement of animal cells

The oxygen requirement r of animal cells is relatively low in comparison with that of microorganisms, with values in the range from $rX \approx 5$–150 mg/l h for a cell concentration $X = 10^7$ cells/ml (see Table 1). Variation of the respiration rate r with the oxygen concentration c in the fermentation solution is observed only below $c/c^* = 10$–20% (c^*: oxygen saturation concentration for air at $p = 1$ bar). Experi-

Table 1. Oxygen demand rX of 10^7 cells/ml and optimal O_2 - concentration c/c^* for fermentation of mammalian cells.

Cell line	rX	c/c^*	Lit
	[mg/l·h]	[%]	
He La	150		
Diploid embryo	48	–	[2]
Baby hamster kidney	36		[3]
	60	> 10	–
Human hybridoma	5	37.5	
Mouse MAK 33	30	–	[4]
Hybridoma SP2/0	61	5–60	[5]
A10 G10	60	> 10	–
Bowes melanoma	22–32	60–85	[6]

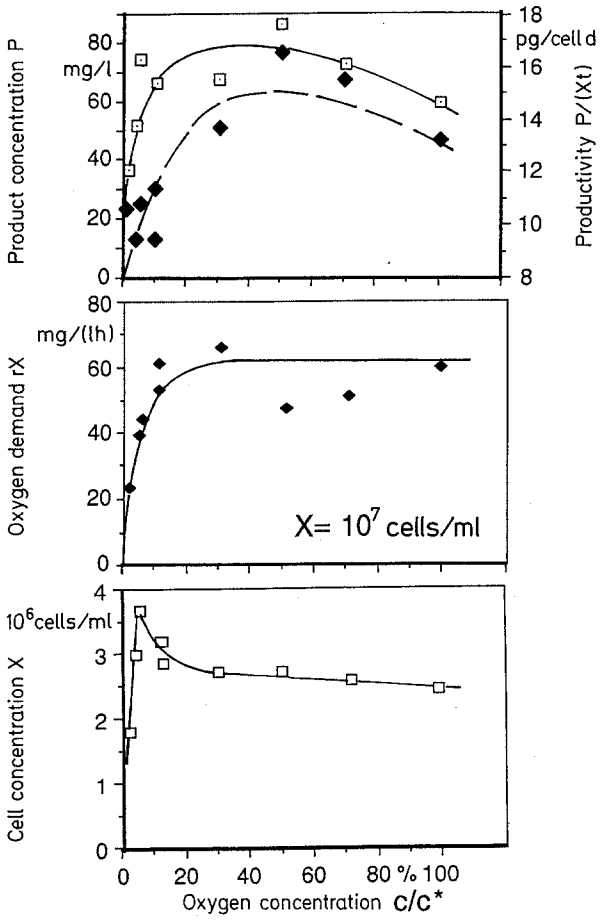

Fig. 1. Influence of oxygen concentration c on continuous fermentation of Mouse hybridoma; P: product concentration, P/Xt: productivity, rX: oxygen demand, X: cell concentration, $c^* = 6.5$ mg O_2/l, oxygen concentration c/c^*

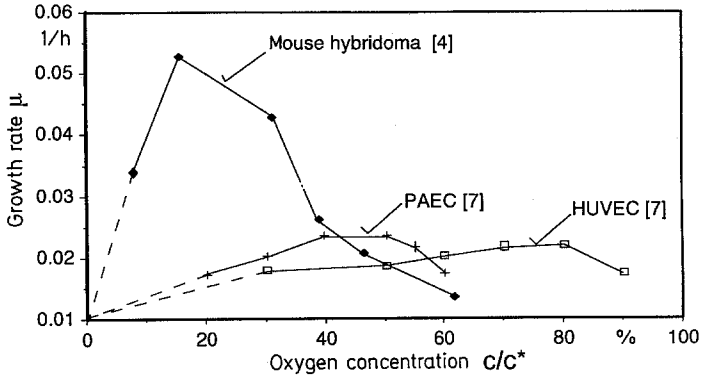

Fig. 2. Influence of oxygen concentration c on growth rate μ of animal cells; $c^* = 6.5$ mg/l; PAEC: porcine aorta cells; HUVEC: Human endothelial cells

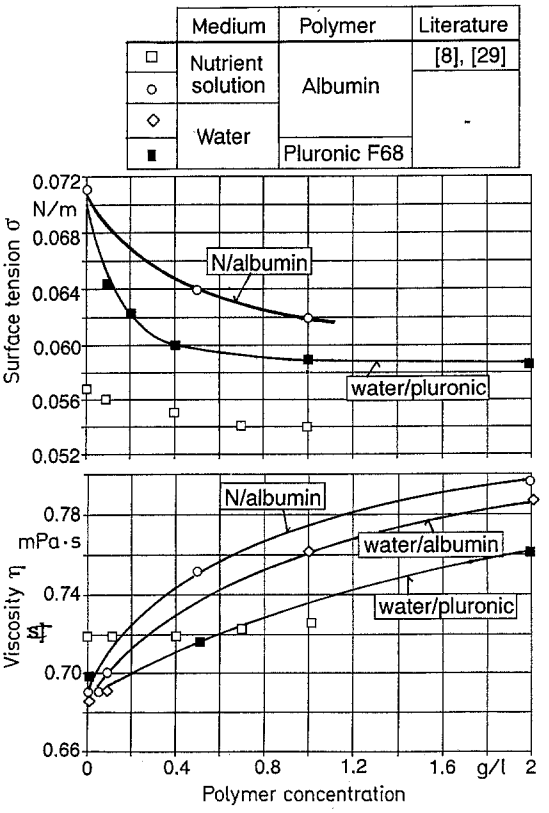

Fig. 3. Influence of polymers on surface tension σ and viscosity η, $\vartheta = 37\,^\circ$C, N: nutrient solution

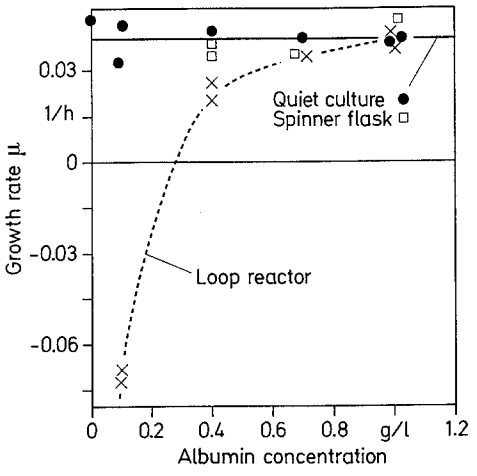

Fig. 4. Influence of Albumin concentration on growth rate μ; medium: Iscove's Dulbecco's/Ham's F 12 : 1 : 1; results from [8], [29]

ence so far indicates that the optimum conditions for growth, cell concentration, and viability as well as product formation are achieved with $5\% < c/c^* < 80\%$ (see Table 1, Figs. 1 and 2).

2 Properties of the nutrient solutions

The properties of the fermentation solutions are not precisely known, since they change very quickly under non-sterile conditions, and are therefore difficult to measure directly. However, rough values can be obtained from

nutrient solutions. The O_2-saturation concentration of a typical nutrient solution (1:1 mixture of Dulbecco's Egale/Ham's F12 with 0.3 g/l of albumin) at $\vartheta = 37°C$ and $p_{O_2} = 0.21$ bar was found to be 6.5 mg of O_2/l, which corresponds to about 95% of the value for pure water.

The viscosity and the surface tension of the nutrient solutions vary slightly with the albumin content (see Fig. 3). Added synthetic polymers such as Pluronic F68 lead to similar changes in the properties.

The presence of albumin has a positive influence on cell growth behaviour whenever increased shear is present in the bioreactor (see Fig. 4). However, an accompanying disadvantage is the negative effect of albumin on gas/liquid mass transfer (see Figs. 13 and 17). Synthetic polymers have similar effects on these properties.

3 Description of tests and measurement methods

Oxygen transfer was determined in reactors having capacities of 2.5 to 800 l. To ensure that coalescence effects in industrial equipment were correctly taken into account, only test plants having a diameter $D \geq 0.4$ m and filling heights $H \geq 0.8$ m were used for bubble aeration in stirred tanks, bubble columns, and loop reactors. Water alone, water containing Pluronic, and nutrient solutions with and without albumin were used as test liquids.

A dynamic method and a steady state method were used for the determination of mass transfer coefficients. The steady state method used was a pumping method with two reactors, in which the oxygen was introduced in the reactor under investigation and driven off in the second reactor. This method was used preferentially in the investigation of membrane reactors with diffusion membranes, since the same oxygen concentration can always be maintained here as in the bioreactor. It is thus possible to determine how supersaturation at the membrane interface affects mass transfer under realistic conditions (see Sec. 6). Supersaturation at the membrane interface is always observed when the membrane pressure is higher than the reactor pressure. The theoretical saturation concentration corresponding to the pressure inside the membrane was always used here for calculation of the mass transfer coefficients $k_L a$.

4 Oxygenation methods

The main oxygenation methods for submersed cultivation of animal cells are shown in Fig. 5. In addition to surface oxygenation and oxygenation via membranes, which produce little mechanical stress, direct aeration in bubble columns, loop reactors, and stirred tanks is also used. The membranes used for oxygenation are mainly open-pore Accurel-membranes and silicone diffusion membranes. The use of open-pore membranes calls for pressure regulation such that the gas/liquid interface remains inside the pores (see Fig. 9), so that no bubbles emerge into the liquid [9]. Non-reinforced and more pressure-resistant reinforced silicone tubes and silicone-coated tubular membranes are used as diffusion membranes [10, 11].

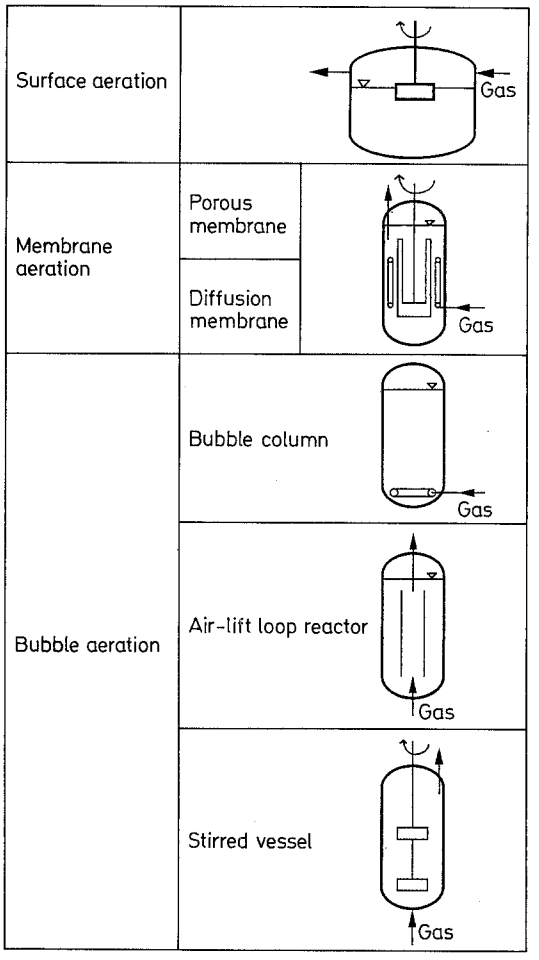

Fig. 5. Methods of oxygen supply for submers fermentation of animal cells

The oxygen supply is determined only by the gas-liquid mass transfer. The additional resistances in the boundary layer on the gas side and on the cell or cell agglomerate side just as in the agglomerates themselves are negligible. The gas–liquid mass transfer can therefore be calculated from the following equation:

$$G/V = ka\Delta c \ . \tag{1}$$

Since the mixing of the liquid phase is generally ideal and the change of concentration in the gaseous phase is only very small, the concentration difference Δc that drives the process is given by:

$$\Delta c = c^* - c \ , \tag{2}$$

where $c^* = p_{O_2}/Hy$ in Eqs. (1)–(2) G/V is the mass flow G referred to the reactor volume V, k is the overall mass

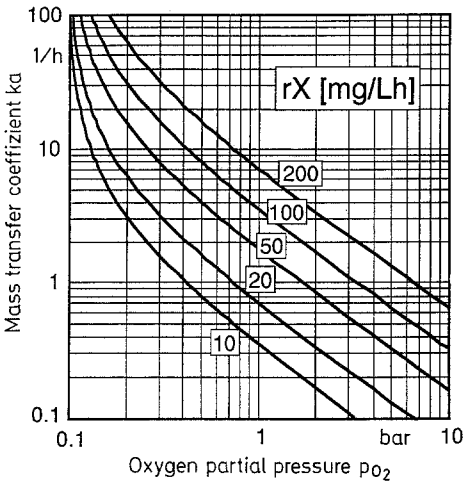

Fig. 6. Required mass transfer coefficient ka as function of oxygen partial pressure; $Hy = 3.2 \cdot 10^6$ Nm/kg, $c = 3$ mg/l

transfer coefficient at the phase interface A, $a = A/V$ was the specific interfacial area, which corresponds to the area of the membrane in membrane oxygenation, and to the area of bubbles in bubble aeration, c^* is the saturation concentration, c is the actual concentration of the relevant gas in the liquid, p_{O_2} is the O_2 partial pressure, and Hy is the Henry coefficient.

To intensify mass transfer, the aeration should be carried out with pure oxygen, and at raised pressures if possible. Under these conditions, according to the general mass transfer Eq. (1), a given oxygen requirement $rX = G/V$ can be satisfied with lower mass transfer coefficients ka, and cell cultivation can be achieved with less shear (see required ka values in Fig. 6).

For the layout of the reactors, it is necessary to know the mass transfer coefficients ka, which must be determined empirically. Since the majority of the existing data are invalid for the low mass transfer coefficients desired in cell fermentation, special investigations were conducted in the various reactors.

5 Surface aeration

In surface aeration, mass transfer occurs only through the surface of the liquid. For the best conditions, an impeller should be located at the interface itself. Investigations with various impellers have shown that the standard disc impeller with 6 blades produces strong surface agitation. Increasing the number of blades and setting the blades at an angle leads to poorer mass transfer.

For wave motion of the surface the effective phase interface is greater than the surface area of the liquid and it becomes appropriate to use the product $ka = k_L a$, which can be easily determined by experiment. Zlokarnik's [13] investigations of surface aerators in sewage purification

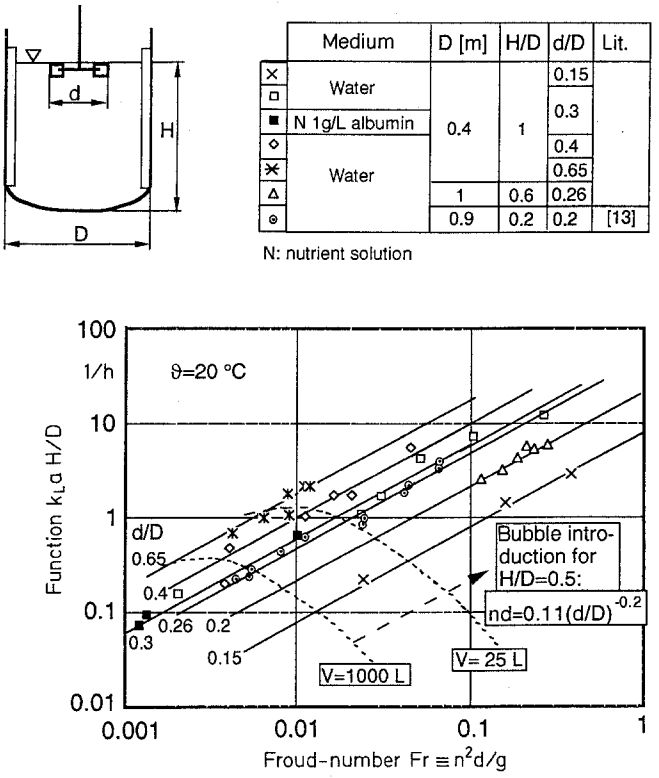

	Medium	D [m]	H/D	d/D	Lit.
×	Water	0.4	1	0.15	
□				0.3	
■	N 1g/L albumin			0.4	
◇	Water			0.65	
✳		1	0.6	0.26	
△		0.9	0.2	0.2	[13]
⊙					

Fig. 7. Sorption characteristic for surface aeration in stirred vessels and limiting curves for the start of bubble introduction

suggest that the product of the mass transfer coefficient and the slenderness ratio $k_L a\, H/D$ should be introduced as the target parameter. For any given substance system, this parameter will depend generally on the impeller diameter d and shape, the impeller speed n and the acceleration due to gravity g. The results in the low power input range can be described by the following simple sorption characteristics (see Fig. 7):

$$k_L a \frac{H}{D} = f\left(\frac{d}{D}\right)\frac{n^2 d}{g} \tag{3}$$

where

$$f\left(\frac{d}{D}\right) = \left(\frac{d}{D} - 0.13\right)\cdot 400, \quad \frac{d}{D} > 0,15 \tag{4}$$

The dependence $f(d/D)$ is not a simple exponential function as found by Zlokarnik [13] for small diameter ratios. The relation $f(d/D) = (d/D)^3$ reported in [13] is verified only for $d/D \leq 0.3$. The influence of the ratio d/D decreases as its magnitude increases (see Fig. 8).

Because bubble introduction should be avoided, oxygen input cannot be increased indefinitely by surface aeration, as is shown by the sorption characteristic. According to the experimental findings, the limiting condition for bubble incorporation is given by the simple relation

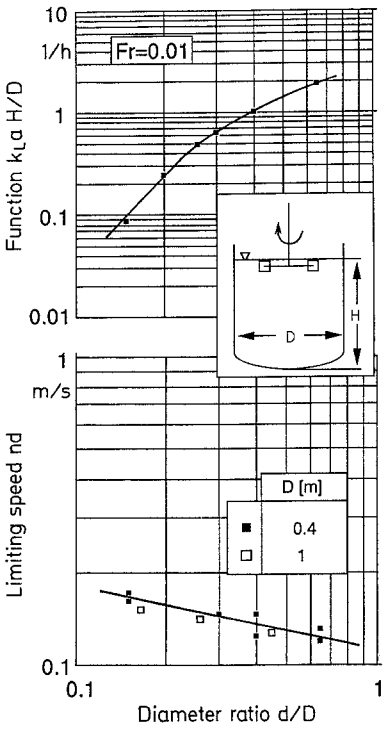

Fig. 8. Influence of diameter ratio d/D on mass transport by surface aeration (upper diagram) and limiting speed nd for beginning of bubble introduction (lower diagram); water/air, turbine impeller

$(Fr \cdot We) \sim nd = \text{constant}$. From investigations with disc impellers located at the surface of the liquid in vessels having $D = 0.4$ and 1 m, the condition for the start of bubble incorporation in water was found to be given by (see lower part of Fig. 8):

$$nd = \frac{0.11[\text{m/s}]}{(d/D)^{0.2}} \quad . \tag{5}$$

Because of the decreasing influence of d/D on the sorption characteristic, there is an optimum diameter ratio, $d/D \approx 0.5$ at which maximum mass transfer can be achieved without bubble introduction (see limiting curves in Fig. 7). For surface aeration, Eqs. (3) and (5) lead to the following scale rule, which is however unfavourable for scale-up:

$$\frac{(k_La)_G}{(k_La)_M} = \frac{H_M}{H_G} \sim \left(\frac{(H/D)_M}{(H/D)_G}\right)^{2/3} \left(\frac{V_M}{V_G}\right)^{1/3} \quad . \tag{6}$$

This relationship holds for $V = 25$ and 1000 l according to Fig. 7, which, in addition to the sorption characteristic, also shows the limiting curves for the start of bubble introduction. Even on the semi-industrial scale, according to this diagram, sufficient oxygenation for cell cultures can no longer be provided via the surface of the liquid. In surface aeration, mass transfer is not affected by additives and proteins such as are used in nutrient solutions (see data points in Fig. 7).

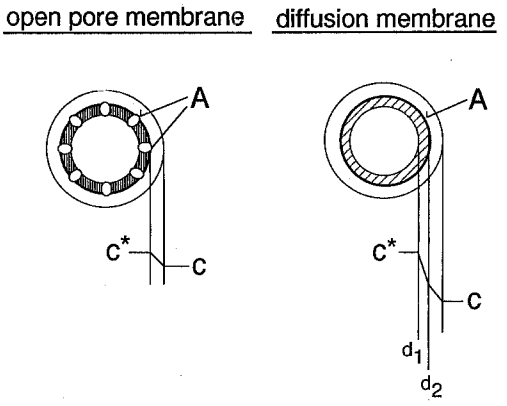

Fig. 9. Concentration profiles for oxygen supply via membranes

6 Membrane aeration

Membrane aeration with open-pore membranes or diffusion membranes is used for low-shear oxygenation of animal cells (see Fig. 9).

In the case of oxygenation with open-pore membranes, in Eq. (1) k is equal to k_L, the mass transfer coefficient at the gas-liquid interface, which is held stationary in the pores of the membranes.

In membrane aeration with diffusion membranes, k is an overall mass transfer coefficient that takes into account the mass transfer coefficient at the liquid-side interface of the membrane k_L and a term for additional membrane diffusion. The following relation applies for a tubular membrane having an outside diameter of d_2 and an inside diameter of d_1:

$$k = \frac{1}{\dfrac{1}{k_L} + \dfrac{d_2 \ln(d_2/d_1)}{2\,\mathbb{D}_s Hy/Hy_s}} \quad , \tag{7}$$

where $\mathbb{D}_s$ is the diffusion coefficient in the membrane material, and $Hy_s = p_{O_2}/c_s^*$ is the Henry constant of the membrane material.

Silicone material has particularly favourable properties for oxygen transfer, since its diffusion coefficient is slightly higher than that of water, and the solubility of O_2 in the material is about 4 to 5 times the solubility in water. According to the results of Bräutigam [12], the temperature dependence of the material constant $\mathbb{D}_s\, Hy/Hy_s$ for water in the temperature range $10 \leq \vartheta\,[^\circ\text{C}] \leq 40$ is as follows:

$$\mathbb{D}_s Hy/Hy_s \approx 7.3 \cdot 10^{-9} \exp(0.024\,\vartheta)\,[\text{m}^2/\text{s}] \quad . \tag{8}$$

The following dimensionless relation is suitable for the description of the mass transfer coefficient k_L at the gas/liquid interface and at the surface of the membrane:

$$Sh = f(Re, Sc) \quad .$$

where the Sherwood number $Sh = k_L d_2/\mathbb{D}$ and the

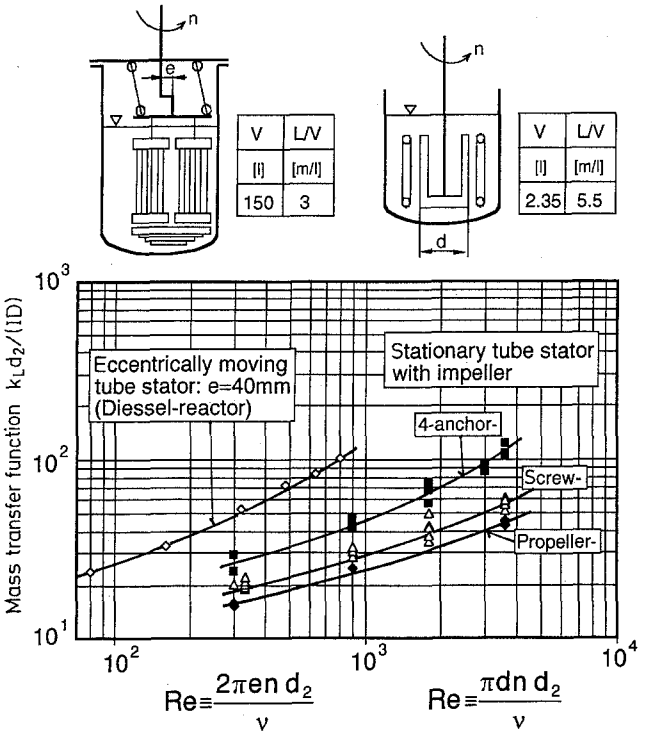

Fig. 10. Mass transfer characteristic for membrane oxygenation, Accurel-membranes, water, $\vartheta = 37\,^{\circ}C$

Reynolds number $Re = ud_2/\nu$ are functions of the characteristic diameter d_2 of the tubular membrane and a characteristic velocity u.

Some experimental results based on $k_L a$ measurements in reactors with open-pore Accurel tubes are shown in Fig. 10 in the form $Sh = f(Re)$. The pore area, which is equal to 75% of the total area and roughly corresponds to the area of the gas/liquid interface, was used here in the determination of the k_L values. Various definitions were used for the Reynolds number, so that direct comparison of the different reactor types is impossible in this form. In the case of the Diessel reactor [9, 14] with an eccentrically moving tube stator, the Reynolds number is derived from the actual velocity $2\pi en$ of the surface of the tube. For a stirred reactor with a stationary tubular basket concentric with the impeller, only the peripheral velocity of the impeller $2\pi dn$ is known, and this was the value used.

In a stirred reactor with a stationary tubular stator, the anchor impeller is found to be the best system, since it produces a more intense and more uniform flow directed towards the tube. This is particularly true comparing impellers of the propeller type, with helical-blade impellers having the same axial length as the anchor impellers used.

For the reactor with a stationary tubular stator and a two-blade anchor impeller, further measurements with water at various temperatures in the range $20 < \vartheta[^{\circ}C] < 37$ gave the following general relation, which was also confirmed by further results with diffusion membranes:

$$Sh = (7.8 + 0.0021 Re^{1.2})\, Sc^{1/6} \quad \text{for}$$

$$250 < Re < 6000 \text{ and } 200 < Sc < 500 \tag{9}$$

The observed dependency on the Schmidt-number is distinctly less than is indicated in the literature for circular cylinders with cross flow [15, 16].

The overall mass transfer coefficient k is required for determination of the dimensions of the oxygenation with diffusion membranes. It can, in principle, be determined mathematically by means of Eq. (7) with the k_L values from the Fig. 10 or Eq. (9), the material constants $\mathbb{D}\, Hy/Hy_s$ from Eq. (8), and the geometry of the tube. Since the diameters and lengths of the tubes in operating condition do not generally correspond to the original dimensions, as a result of the stretching produced by coiling and by pressure, only a rough prediction is possible by this means. Moreover, there are additional effects resulting from supersaturation at the membrane interface, which is to be expected when the concentration at the membrane c_M is greater than the saturation concentration c_R^* corresponding to the O_2 pressure in the reactor $(p_{O_2})_R$:

$$\frac{c_M}{c_R^*} = \frac{Hyc}{(p_{O_2})_R}\left(1 - \frac{k}{k_L}\right) + \frac{p_{O_2}}{(p_{O_2})_R}\frac{k}{k_L} > 1 \tag{10}$$

According to Eq. (10) this is particularly likely when the O_2-concentration c in the liquid phase is high, when the pressure in the membrane p_{O_2} is higher than the pressure in the reactor $(p_{O_2})_R$, and when the ratio k/k_L is high, i.e. when the membrane is thin and there is little movement at the membrane surface.

Supersaturation leads to the formation of microbubbles, which rise to the surface of the liquid once they reach a certain size with the result that mass transfer is adversely affected (see upper part of Fig. 11). In the case of non-reinforced membranes, this effect is more than offset by the stretching of the tube and the resulting decrease in the wall thickness (see lower part of Fig. 11).

As was shown above, mass transfer can be distinctly improved by selection of a suitable impeller system (see Fig. 12). The anchor impeller developed especially for membrane aeration is clearly superior to the conventional axial impellers (propeller and pitched-blade impellers) that are frequently described in the literature and recommended by manufacturers. With these impellers, the k values were also found to decrease with increasing coiling tightness, owing to the non-uniform movement in the reactor. They require much higher speeds and power inputs, with the result that shear on the cells is increased. For increasing coiling tightnesses $L'/V \approx 1.9$ m/l, a pitched-blade impeller, for example, requires more than 2 to 5 times as much power as the recommended anchor impeller in order to produce the same mass transfer.

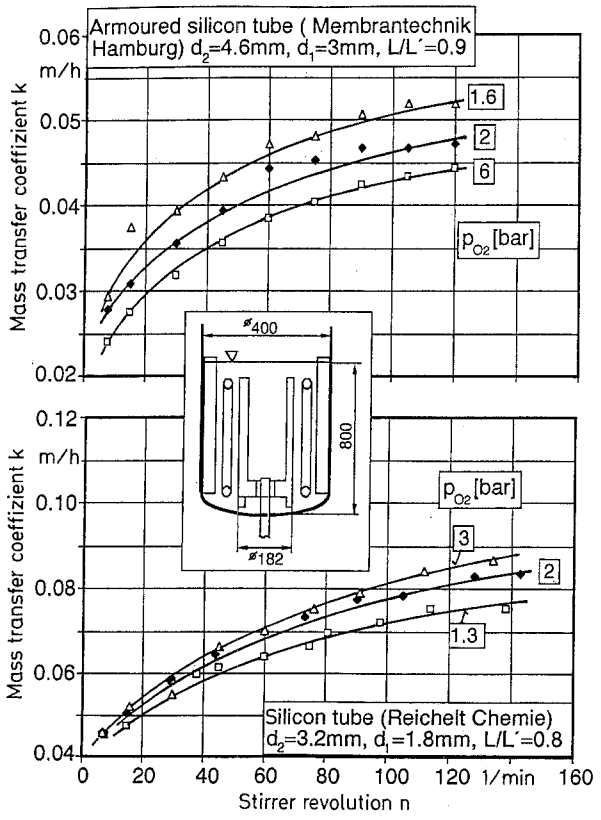

Fig. 11. Mass transfer coefficients for diffusion membranes, 2-anchor impeller, water, $\vartheta = 35\,°C$ $(p_{O_2})_R = 0.21$ bar, $c = 3$ mg/l

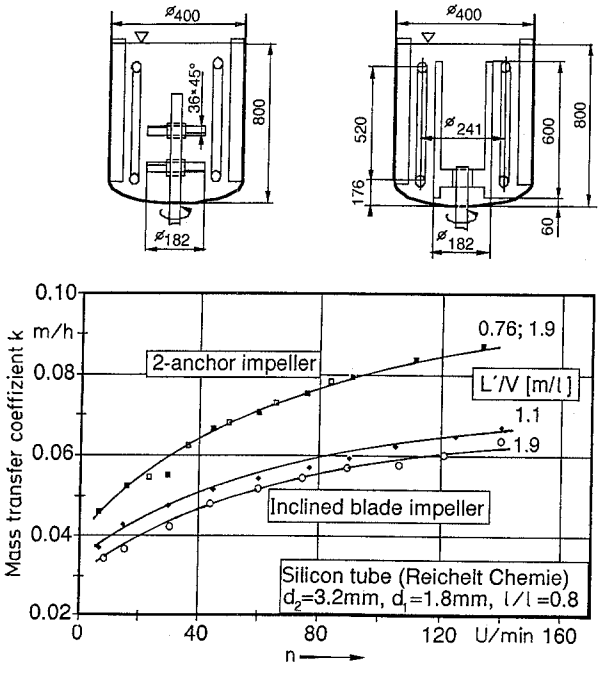

Fig. 12. Influence of impeller system on mass transfer coefficient, water, $\vartheta = 35\,°C$, $p_{O_2} = 3$ bar, $(p_{O_2})_R = 0.21$ bar, $c = 3$ mg/l, $\frac{L}{L'} = 0.8$

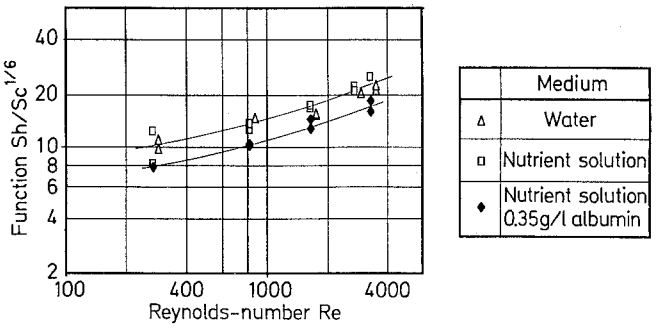

Fig. 13. Influence of medium composition on mass transfer; Accurel-membrane; screw impeller with 4 bars

In the case of open-pore Accurel membranes, lower k_La values were found in nutrient solutions containing albumin than in water (see Fig. 13); this is analogous to the values indicated in Fig. 17 for bubble aeration. As will be shown in the following sections, this can be explained by additional diffusion resistance at the bubble surface due to the presence of protein. In the case of diffusion membranes no negative effect on mass transfer was observed.

7 Bubble column

For a specified system of substances, specified dimensions for diameter and height of reactor and a specified type of sparger, the mass transfer coefficient k_La in bubble columns and loop reactors depend only on the superficial gas velocity v. The relation

$$k_La = Bv^b \tag{11}$$

applies with the exponent b a further function of the superficial velocity (see Figs. 14 and 15). The influence of the diameter of the sparger holes is particularly noticeable at low gas velocity in the range desired for the oxygenation of cell cultures. With increasing gas velocity, the ratio k_La/v, which is a measure of the aeration efficiency, i.e. of the utilization of the gas, decreases as a result of increasing coalescence (see Fig. 15); it is therefore advisable to use oxygen-enriched air in order to minimize shear due to gas bubbles, particularly in the case of direct aeration. An exception is found in large-bubble aeration with hole diameters ≥ 2 mm in the mid-range of gas velocities ($10 < v\ [m/h] < 60$). With increasing gas flow make the distribution of the gas over all the sparger holes becomes increasingly uniform, and this leads to reduced coalescence because of the decrease in the local gas hold-up.

As was already mentioned mass transfer is clearly hindered in nutrient solutions containing albumin (see

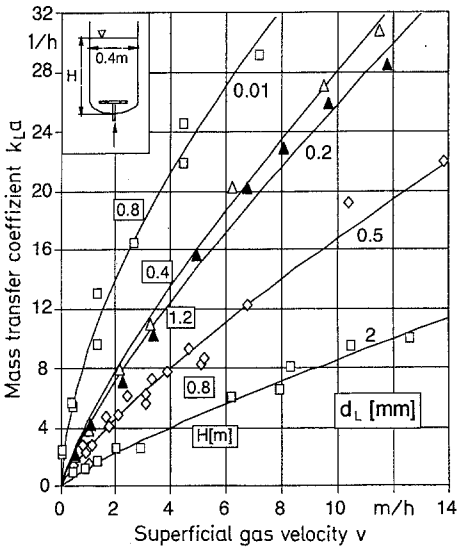

Fig. 14. Volumetric mass transfer coefficient for bubble columns, water, $\vartheta = 35\,°C$

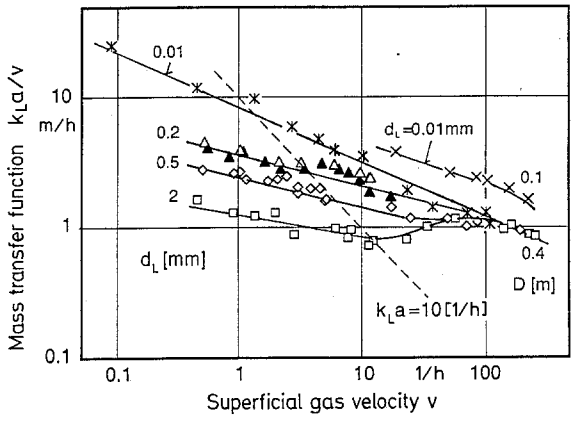

Fig. 15. Related mass transfer coefficients for bubble columns: Influence of sparger and column diameter; $H > 0.8$ m, water, $\vartheta = 35\,°C$

Figs. 13, 16 and 17). Only about 10% of the observed difference can be explained by the influence on the viscosity, according to the following dimensionless correlation, which also follows from Eq. (14) for $P = 0$, and which gives a sufficiently accurate representation of the influence of the viscosity (see [17–19]) on mass transfer:

$$Y_1 = \frac{k_L a}{v}\left(\frac{\nu^2}{g}\right)^{1/3} = f\left[\frac{v}{(\nu g)^{1/3}}\right] \qquad (12)$$

From this result and those given in Fig. 16 and Table 2, according to which the intensity of the effect differs with the diameter of the sparger holes, it may be assumed that mass transfer is hindered by the presence of protein at the interface. Increased coalescence of bubbles must be ruled

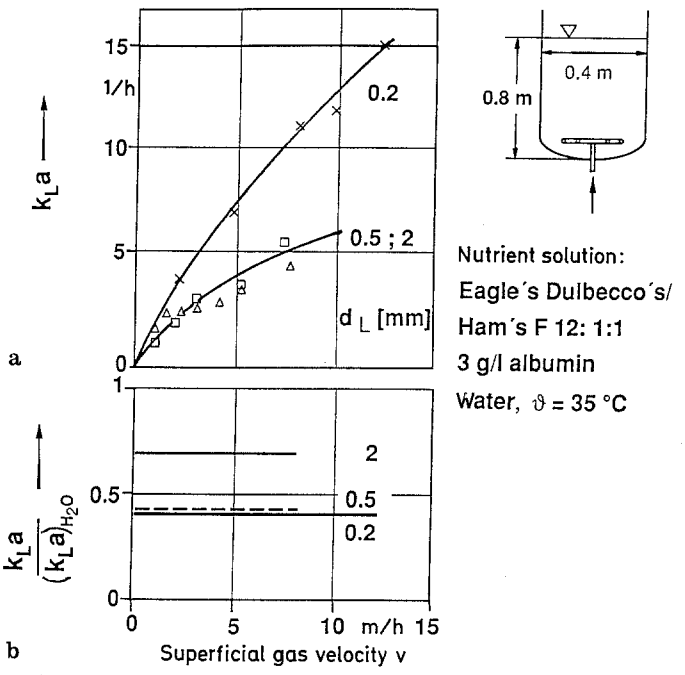

Fig. 16a, b. Mass transfer functions for bubble columns with nutrient solution (*a*) and the comparison with data for water (*b*)

	Reactor	d_L [mm]	Polymer	Literature
■	Air lift	0.2	Albumin	[8], [29]
□	Bubble column	<0.25		–
◇		0.2		
◆		0.5		
✳		2		
×	Accurel membrane	$3 \cdot 10^{-4}$		
△	Stirred	2		
▲			Pluronic	

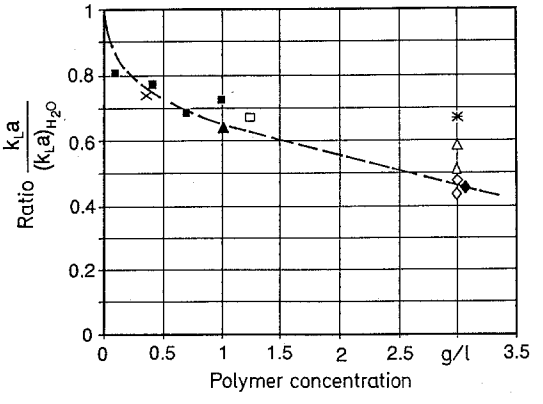

Fig. 17. Influence of polymer concentration on mass transfer ratio

out because a tendency to foam formation is observed in nutrient solutions containing albumin. The greater mass transfer reductions found with small sparger hole diameters ($d_L = 0.2$ and 0.5 mm) indicate that in the case of

Table 2. Sorption characteristics for bubble columns, water:

$$\frac{k_L a}{v}\left(\frac{v^2}{g}\right)^{1/3} = A\left[\frac{v}{(vg)^{1/3}}\right]^{-a}$$

Gas-sparger	d_L[mm]	A	a	$\frac{v}{(vg)^{1/3}}$
Fritte	0.01	$6 \cdot 10^{-5}$	0.4	0.001 – 0,1
	0.2	$6,3 \cdot 10^{-5}$	0.2	
Double ring	0.5	$4.2 \cdot 10^{-5}$		0.01 – 0.2
	2	$2.2 \cdot 10^{-5}$	0.17	

smaller bubbles, because of the rigid interface, the inhibition of mass transfer by protein on the bubble surface is more pronounced than for larger bubbles, where agitation of the bubble surface is produced by increased circulatory flow within larger bubbles. This assumption is reinforced by the results obtained with surface aeration, where mass transfer was found to be totally unaffected by proteins.

8 Loop reactor

For the superficial velocity, related to the total cross section of the reactor, mass transfer must be expected to be lower in a loop reactor than in a bubble column, since only part of the column cross section is aerated and $k_L a$ is less than directly proportional to the superficial velocity. This is confirmed by the experimental results presented in Fig. 18. If it is assumed that the bubble size is the same in both reactors and that the circulation velocity in the loop reactor is always small in comparison with the bubble rise velocity, it then should be possible to calculate the mass transfer coefficients for loop reactors $(k_L a)_c$ from those for bubble columns $k_L a$; the actual superficial velocity v_S in the aerated volume of the loop reactor with the cross section A_s must be used here in the bubble column characteristic:

$$(k_L a)_c = k_L a(v_s)\left(\frac{4A_s}{\pi D^2}\right)^2 \tag{13}$$

As can be seen from the right part of Fig. 18, Eq. (13) allows a rough calculation for the case $k_L a < 6$ [h].

9 Stirred reactor

Gas/liquid mass transfer can be intensified by stirring. The region of low impeller power is of interest for cell culture. As is well known and can be seen from Fig. 19, the $k_L a$ values are independent of the type and geometry of the impeller if sufficient mixing takes place in the reactor. The viscosity of the culture solutions is so low that this condition is practically always satisfied. It is valid

$$k_L a \sim v^b \left(\frac{P}{V}\right)^c \tag{13}$$

From Fig. 19 it may be deduced that a given mass transfer will be achieved at much lower impeller speeds with large radial transport impellers than with small impellers such as the standard disc impeller with $d/D = 0.33$ or propeller and pitched blade impellers, which also have distinctly lower Newton-numbers Ne (see e.g. [20]) than radial impellers. Moreover, the mass transfer coefficients obtained at low impeller powers ($P/V < 25$ W/m^3) are distinctly lower in the case of the disc impeller, since the bubbles are no longer uniformly distributed by this impeller, and some of them strike the horizontal impeller disc, with the result that coalescence is intensified.

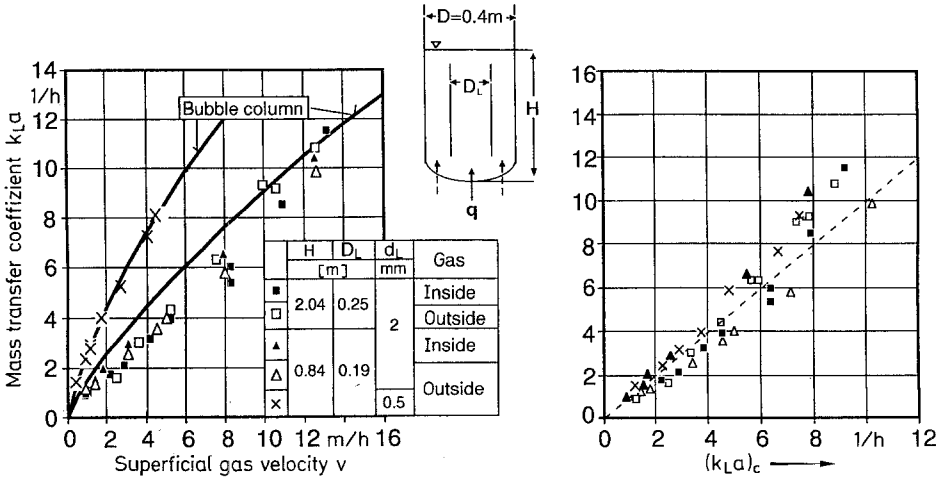

Fig. 18. Mass transfer coefficients $k_L a$ for air lift reactors as function of superficial gas-velocity $v = 4\ q/\pi D^2$ (left diagram) and comparison of measured $k_L a$ with Eq. (12) calculated data $(k_L a)_c$ (right diagram), water $\vartheta = 34\,^\circ$C

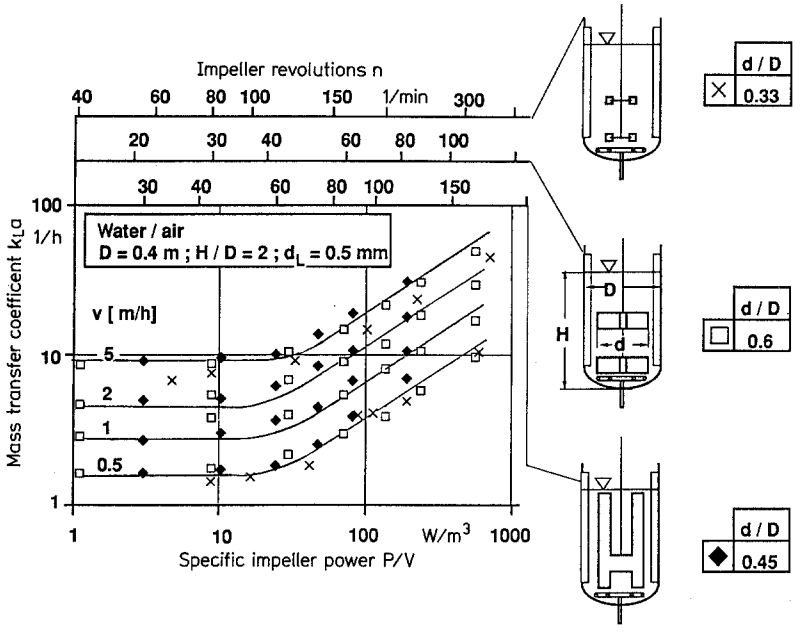

Fig. 19. Mass transfer coefficient k_La for various superficial gas velocities v and specific impeller power P/V or impeller revolutions n in stirred vessels, $\vartheta = 35\,°C$

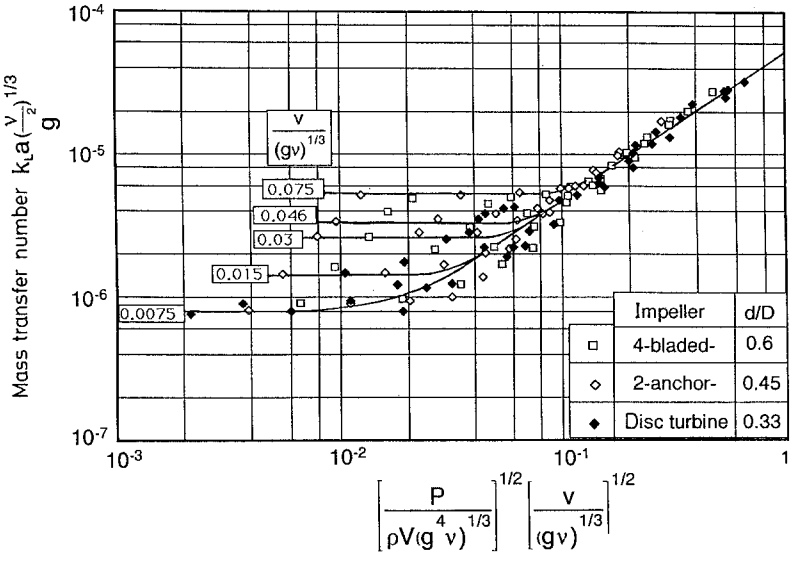

Fig. 20. Sorption characteristics for stirred reactors: Dimensionless representation of data from Fig. 19

The k_La values for a given two-phase system can often be described by the following dimensionless correlation [19]:

$$Y_2 = k_La\left(\frac{v}{g^2}\right)^{1/3} = f\left[\frac{V}{(gv)^{1/3}};\ \frac{P}{\rho V(g^4 v)^{1/3}}\right] \tag{14}$$

Figure 20 shows the correlation of the results in Fig. 19 that can be achieved in this manner for higher impeller powers. Rearrangement leads to a simple relation similar to that reported by Henzler [19] for the sorption of oxygen in water:

$$Y_1 = \frac{k_La}{v}\left(\frac{v^2}{g}\right)^{1/3} = 4.5\times 10^{-5}\left[\frac{P}{\rho V}\frac{1}{vg}\right]^{1/2} \tag{15}$$

Table 3. Range for validity of sorption characteristics of Eq. (15)

Gas sparger	d_L[mm]	P/V[W/m³]
Fritte	0.01	> 100
	0.5	> 30
Double ring		
	2	> 10

The range over which this relationship may be used depends on the sparger type (see Table 3). Low stirrer power result in bubble column operation, for which the sorption characteristics given in Table 2 are valid.

An additional dependence on the Schmidt-number need only be considered for the sorption of a gas (b) other than oxygen (a). In this case the sorption characteristics must be corrected in the following manner: $Y_b/Y_a = (Sc_a/Sc_b)^c = (\mathbb{D}_b/\mathbb{D}_a)^c$. For the agitated interfaces, which are present for larger bubbles with diameters > 2.5 mm, the exponent c is 0.5 (see Calderbank [21]).

As in fine-bubble aeration in bubble columns and loop reactors, the presence of albumin in nutrient solutions leads to a decrease in the sorption parameter, i.e. in the gas transport (see Fig. 17). The synthetic polymer Pluronic F68 has a similar effect.

10 System comparison

10.1 Aeration performance comparison

The attainable mass transfer coefficient k_La or the oxygen input per unit volume G/V will be taken as the target parameter. The comparison of the various reactors will be carried out as a function of the maximum velocities u in the reactors or the specific impeller powers P/V.

The calculated results obtained from the sorption characteristics reported are valid for a gas of pure oxygen, a typical nutrient solution containing 1 g/l albumin (according to the data of Fig. 17 a 35% impairment of mass transfer is to be expected when O_2 is supplied via open pore membranes or by sparging) and a temperature of $\vartheta = 37\,°C$, with the corresponding material parameters $Hy = 6.2 \cdot 10^6$ Nm/kg, $\nu = 0.8 \cdot 10^{-6}$ m^2/s, $\mathbb{D} = 3.2 \cdot 10^{-9}$ m^2/s.

In the case of membrane oxygenation the calculations were performed for a total membrane area of $A/V = 25$ m^2/m^3. For open pore membranes only 75% and reinforced membranes 90% of this area has to be taken as effective. The used total membrane area requires the installation of 1.75 - 3.06 m tubing/l reactor volume, depending on the diameter of the tubing (see Table in Fig. 21). This is near the limit of technical feasibility for stirred vessels. From these data it is clear that the use of membranes necessitates complex reactor structures that would be more likely to malfunction than sparged fermenters.

10.1.1 Bubble free aeration

Figure 21 shows the attainable mass transfer coefficient ka and the oxygen input G/V as functions of the maximum velocity u taken as tip speed of basket (Diessel - reactor) or impeller. Oxygenation via the surface of the liquid does not provide sufficient oxygen transfer, even with low height-to-diameter ratios H/D. From the standpoint of the supply of O_2, the open-pore Accurel membrane combined with the Diessel reactor offers the best solution. However, this reactor has not proved to be practical for large scale systems, because of its complicated technology and the danger of hydrophilization of the Accurel membranes, which would cause cells to grow on the membrane.

The low efficiency of aeration techniques with diffusion membranes can be improved by the use of higher gas-side pressures (see Fig. 22). Oxygen inputs G/V of 130 to 180 mg/l can then also be achieved with silicone membranes.

The comparison in Fig. 22 was conducted with stable diffusion membranes having a relatively thick wall. By reduction of the wall thickness, it is possible to reduce the diffusion resistance of the membrane in accordance with Eq. (7), but less gas pressure can then be realized in the tube; there is thus an optimum tube geometry for the maximum oxygen transfer per unit area of membrane G/A. Stress tests show that commercially obtainable non-reinforced silicone tubes can be exposed to a pressure of

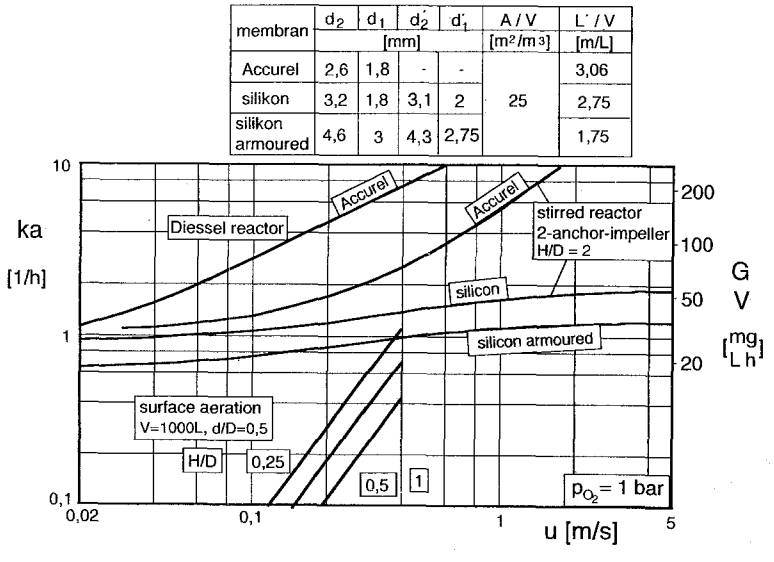

Fig. 21. Comparison of different methods of bubble free oxygen supply mass transfer coefficients ka and possible oxygen supply G/V for $Hy = 3.2 \cdot 10^6$ Nm/kg, $c = 3$ mg/l, $\vartheta = 37\,°C$

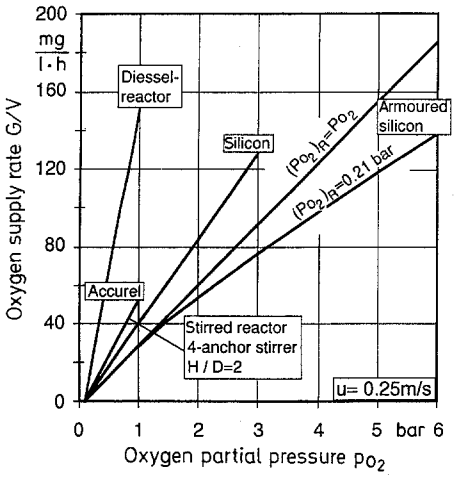

Fig. 22. Oxygen uptake in different membrane reactors, $Hy = 3.2 \cdot 10^6$ Nm/kg, $c = 3$ mg/l, $\vartheta = 37\,^{\circ}C$, tube dimensions see Fig. 21

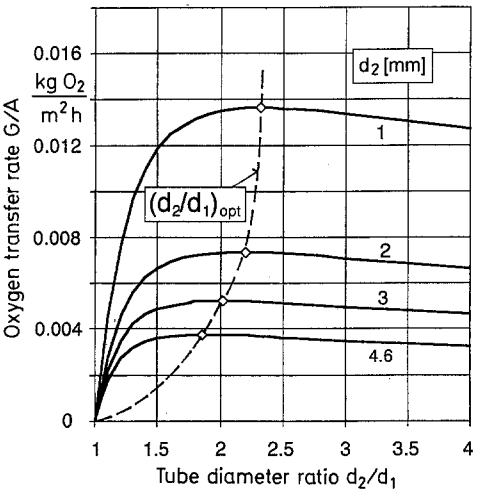

Fig. 23. Influence of silicon tube geometry on O_2-transport corresponding to Eq. (16), $Hy = 3.2 \cdot 10^6$ Nm/kg, $c = 3$ mg/l, $\vartheta = 37\,^{\circ}C$

$p_{adm} \approx 2\sigma_{adm}\,(1\text{-}d_1/d_2)$ with $\sigma_{adm} = 4 \cdot 10^5$ N/m^2. The flow per unit area G/A with the highest possible pressures p_{adm} inside the tube is thus found to depend on the geometry of the tube as follows:

$$\frac{G}{A} = k(c^* - c) = k\left(\frac{p_{O_2}}{Hy} - c\right)$$

$$= \frac{2\sigma_{adm}(1 - d_2/d_1) - c}{Hy\left(\frac{1}{k_L} + \frac{d_2 \ln d_2/d_1}{2\,\mathbb{D}Hy/Hy_s}\right)} \qquad (16)$$

The mass transfer coefficient k_L for the boundary layer on the membrane according to Figs. 11 and 12 and Eq. (9) also depends on the outside diameter d_2 of the membrane. The illustratively calculated results presented in Fig. 23 show flat optima for the mass flows G/A, which move towards smaller diameter ratios with increasing outside diameter d_2. The mass transfer can be distinctly improved by the use of so-called micro-silicone tubes. However, a disadvantage of these tubes is its difficult handling and the greater pressure loss of the gas flow, which makes it necessary to divide the tube into several parallel segments. Not only is this technically more complicated, but it also leads to reduced reliability because of the greater number of gas connections. As is shown in Fig. 24 therefore, micro-silicone tubes are impracticable even for semi-industrial plants.

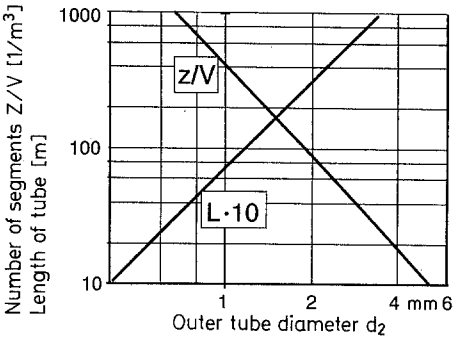

Fig. 24. Number of required segments z per fermenter volume V and length L of silicon tube per segment for a pressure drop of 0.5 bar; valid for optimal tube dimensions given in Fig. 23; G/V = 125 mg/lh; oxygen depletion 10%; further data see Fig. 23

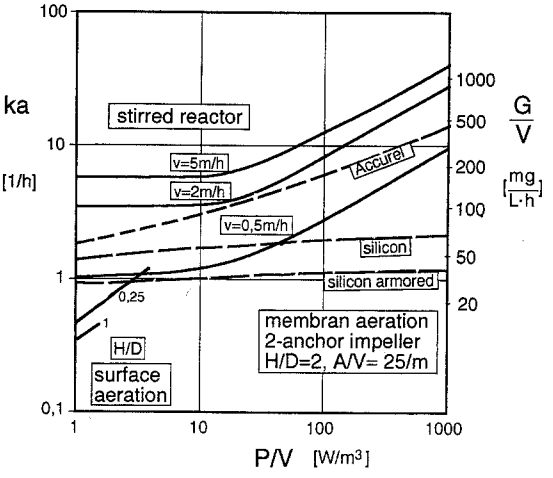

Fig. 25. Comparison of bubble free oxygen supply and sparged oxygen supply: Mass transfer coefficient ka and possible oxygen supply rate G/V; conditions see Fig. 21

10.1.2 Direct sparging

Figure 25 shows a comparison of direct aeration with the bubble-free oxygenation methods. Even at normal pressure, bubble columns and stirred tanks allow sufficient oxygen transfer through aeration and/or stirring, so that there is also no problem in connection with the elimina-

tion of CO_2. With very low gas throughputs of e.g. $v = 2$ m/h, an oxygen input G/V of 200 mg/lh can be achieved with a specific impeller power $P/V \approx 80$ W/m^3. As was shown in Section 9, the nature of the impeller system is of no importance. No definite answer can be given at present to the frequently raised question concerning that type of impeller that produces particularly low shear for a given power input, and are therefore particularly suitable. However, the following considerations do provide information on the influence of stirrer size, reactor geometry and reactor size.

10.2 Comparison with regard to mechanical stress

10.2.1 Notes on mechanical stress

Mechanical stress arises from the movement of the liquid in the reactor, which is essential for mixing, suspending, and gas/liquid mass transfer, and which is produced by an impeller and/or by rising gas bubbles.

Since densities of microorganisms, cells, and even carriers with cells growing on them are only very slightly different from the density of the nutrient solution, these particles follow the mean movement of the liquid with practically no slip. Mechanical stress τ must therefore be assumed to result mainly from the frequent turbulent velocity fluctuations:

$$\tau \sim \rho \overline{u'^2} \tag{17}$$

From statistical theory of turbulence (see Hinze [22]), according to which turbulence can be explained by eddies of various sizes and having energies that decrease with their size, shear must be due mainly to the eddies having sizes similar in size to those of the particles. Distinctly larger eddies follow these like a convective motion, while smaller eddies are too weak to be of any importance. Because of the low power input ($P/V \approx 1$ to 100 W/m^3), the particles contained in the cell culture are generally smaller than the smallest turbulence elements, so that these are the only elements that can be critical. In the velocity field of these eddies, the particles are subjected to shear or to a dynamic stress as a result of the continuous formation and disappearance of eddies, which have a very short life time. For isotropic turbulence these are the eddies in the dissipation range of the turbulence spectrum, for which $\sqrt{\overline{u'^2}} = 0.26\, dp \sqrt{\varepsilon/\nu}$ (see e.g. Hinze [22]; Liepe [23]) and thus Eq. (17) yields the following relation for the shear:

$$\tau_1 \sim \rho \overline{u'^2} \sim \rho d_P^2 \frac{\varepsilon}{\nu} . \tag{18}$$

Because of the non-uniform energy distribution in the reactors, the particles experience different stresses as they circulate within the reactor. The maximum value of the energy dissipation ε is of interest for the determination of the maximum stress. If the cells are not destroyed during a single transit through this region, the viability of a culture will also depend on the frequency with which the maximum stress occurs and the time spent in the zones of maximum energy density. It must therefore also be expected to depend on the pumping capacity of the impeller and the ratio of the impeller volume to the reactor volume).

The maximum energy density differs very considerably from the mean energy dissipation $\bar{\varepsilon} = P/\rho\, V$. Möckel [24] has found the following relation for disc impellers:

$$\varepsilon \approx \frac{0.47(H/D)}{(d/D)^3 (h/d)} \bar{\varepsilon} \quad \text{for} \quad 0.25 < d/D < 0.5 \tag{19}$$

Most of the results of measurements by Laufhütte [25], who also investigated axial-transport impellers such as propeller and inter-MIG impellers, can also be described by this relation if a value of 0.32 is used for the constant instead of 0.47. Geissler [26], on the other hand, found a different correlation for similar impeller types:

$$\varepsilon \sim \frac{(H/D)}{(d/D)^3} \mathrm{Ne}^{1/3} \bar{\varepsilon} \quad \text{for} \quad 0.3 < d/D < 0.7 \tag{20}$$

Whereas the dependence $\varepsilon \sim (d/D)^{-3}$ is confirmed by all of the experimental results, the Eqs. (19) and (20) give very different pictures for the influence of the impeller type. In contrast with Laufhütte's results, impellers having small Newton-numbers are preferable according to Geissler. In particular, these include axial-transport impellers.

In view of the contradictions between the results obtained so far, together with the unanswered question whether they apply to all impeller systems, and also the lack of information on the energy dissipation distribution in bubble columns, it is impossible at present to make any generally valid assessment of the various bioreactors on the basis of the shear hypothesis after Eq. (17). The relation $\sqrt{u'^2} \sim u$, which is generally valid for a given type and geometry of reactor, must therefore be used for the identification of fundamental dependences on the slenderness and size of the reactor. The shear according to Eq. (16) can thus be estimated from the maximum velocity u present in the reactor:

$$\tau_2 \sim \rho \overline{u'^2} \sim \rho u^2 \tag{21}$$

According to the available experimental results (see e.g. Handa [27]; Tramper [28]; Hülscher [29]), an additional and particularly undesirable effect must be attributed to aeration as far as shear on animal cells is concerned. It is assumed that damage by gas bubbles is caused by the forces that occur during the formation or bursting of the bubbles at the surface of the liquid or by direct contact between the cell membrane and the bubbles. Regardless of the mechanism responsible, the most important shear resulting from the aeration is proportional to the number of bubbles formed, and hence to the gas throughput per

Table 4. Influence of geometry and reactor size on stress of cells

Reactor	$\tau_1 \sim \frac{\varepsilon}{v}$	$\tau_2 \sim \rho u^2$	$\tau_3 \sim \frac{q}{V}$
Stirred-	$\frac{1}{(d/D)^3}\left[\frac{P}{V}\right]$	$\frac{V^{2/9}}{\left(\frac{H}{D}\right)^{2/9}\left(\frac{d}{D}\right)^{4/3}}\left[\frac{H/D}{Ne}\frac{P}{V}\right]^{2/3}$	
Bubble column-		$\frac{V^{1/3}}{\left(\frac{H}{D}\right)^{1/3}}[\mathrm{v}]$	$\frac{[\mathrm{v}]^{3/4}}{\left(\frac{H}{D}\right)^{2/3}V^{1/3}}$
Air lift-		$\left(\frac{H}{D}\right)^{2/3}V^{1/3}[\mathrm{v}]$	

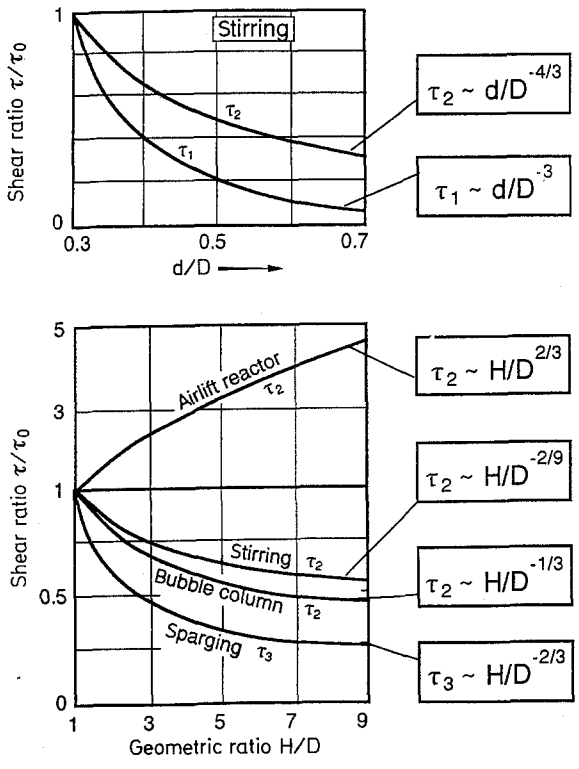

Fig. 26. Influence of impeller and reactor geometry on mechanical stress for v and P/V = constant

unit volume of the reactor q/V, which we shall consider as a third shear hypothesis:

$$\tau_3 \sim \frac{q}{V} \sim \frac{\mathrm{v}}{H} \tag{22}$$

10.2.2 Comparison of sparging methods

The relationships yielded by the three stress hypotheses expressed by Eqs. (18), (21), (22) for the individual types of reactor are given in Tab. 4. If the only effects considered

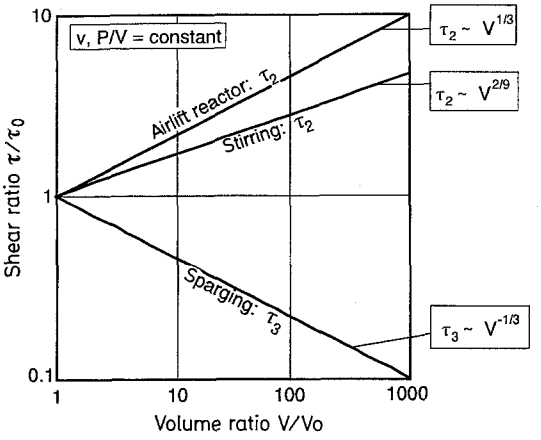

Fig. 27. Variation of mechanical stress with increasing reactor volume

are those of the geometric ratios d/D and H/D, the term $H/D/Ne$ is assumed to be constant in the case of the stirred tank, since the number of impellers is generally proportional to H/D. The relation found by Riquarts [30] for the maximum velocity of the liquid phase in the centre of the column, $u \sim \sqrt{gD}$, was used for the calculation of the velocity in bubble columns. The circulation velocity for loop reactors is given by $u \sim \sqrt{2gH\Delta\varepsilon/\zeta}$; for simplicity, the difference between the gas contents $\Delta\varepsilon$ in the upward and downward flows was taken to be $\Delta\varepsilon \sim v$, and the resistance coefficient of the circulating flow ζ was assumed to be constant.

The relative variation of the mechanical stresses for the case of a constant superficial gas velocity v or a constant specific impeller power P/V, i.e. constant mass transfer, which follows from the relations given in Table 4 is presented graphically in Fig. 26. It shows that it is preferable to use impellers with high ratios of impeller to reactor diameter d/D and slender reactors. The loop reactor is an exception with regard to the motion of the liquid, which increases with the slenderness ratio H/D of the vessel.

Finally, Fig. 27 shows the scale-up relationships. Whereas the velocity of the liquid increases with the size of the reactor, the shear produced by the bubbles simultaneously decreases. If the size of the reactor is increased e.g. from $V = 1$ l to $V = 1000$ l, the main shear due to the aeration decreases by a factor of 10. Moreover, the slenderness ratios in the case of small fermenters are always low, and hence unfavourable with regard to shear, because of the small reactor diameter. This is a very important indication, since the information obtained so far shows that the shear is mainly due to the aeration. It suggests the possibility that problems observed on the laboratory scale are of minor importance in larger reactors, so that possibly aeration can in many cases be used for oxygenation even in production processes with animal cells.

References

1. Henzler, H.-J.; Kauling, J: Sauerstoffversorgung von Zellkulturen. Lecture presented at Fachausschußsitzung. Bioverfahrenstechnik der GVC in Würzburg Mai 1990 and Preprints of 2. Taunustagung in Bad Soden Febr. 1991
2. Thilly, W. G.: Mammalian Cell Technology. Butterworths 1986
3. Bailey, J. E.; Ollis, D. F.: Biochemical Engineering Fundamentals. McGraw-Hill Book Company 1987
4. Brunner, H.; Comer, M. J.; Kearns, M. J.: Preprints of 2. BMFT Statusseminar "Produktion natürlicher Substanzen aus tierischen Zellen" 1985 Herausgeber Bundesministerium für Forschung und Technologie in Bonn
5. Miller, W. M.; Wilke, C. R.; Blanch, H. W.: Journal of Cellular Physiologie. 132 (1987) 524–530
6. Bödeker, B.; u.a.: see 4.
7. Fiedl, P.; u.a.: Different oxygen sensitivities of vascular endothelical cells in an stirred bioreactor. Bericht der GBF Braunschweig
8. Hülscher, M.; Pauli, J.; Onken, U.: Biotechnology Letters. 10 (1988) 689–694
9. Lehmann J.; Piehl, W.; Schulz, R.: Biotech-Forum 2 (1985) 112–117
10. Bräutigam, H.-J.; Sekoulov, I: Forum Mikrobiologie 9 (1986) 269–272
11. Bräutigam, H.: Preprints der 2. Taunustagung Membrantechnologie. Bad Soden 26 27.2.1991
12. Bräutigam, H.-J.: "Untersuchungen zum Einsatz von nichtporösen Kunststoff membranen als Sauerstoffeintragssystem" Dissertation TH Hamburg-Harburg 1985
13. Zlokarnik, M.: Korrespondenz Abwasser 27 (1980) 14–21
14. Vorlop, J.; Lehmann, J.: Chem. Eng. Technol. 11 (1988) 171–178
15. Brauer, H.; Mewes, D.: Stoffaustausch einschließlich chemischer Reaktion" in Grundlagen der Chemischen Verfahrenstechnik. Verlag Sauerländer, Aarau und Frankfurt am Main 1971
16. Perkins, H. C.; Leppert, G.: Trans. ASME C.J. Heat Transfer. 84 (1962) 257–63
17. Henzler, H.-J.: Chem.-Ing.-Tech. 52 (1980) 643–652
18. Zlokarnik, M.: Acta Biotechnologica 1 (1981) 311–325
19. Henzler, H.-J.: Chem.-Ing.-Tech. 45 (1982) 461–476
20. Henzler, H.-J.: VDI-Forschungsheft 587. 1978. VDI-Verlag
21. Calderbank, P. H., Moo-Young, M. B.: Chem. Engng. Sci. 16 (1961) 39–54
22. Hinze, J. O.: Turbulence. Mc Graw-Hill, New York 1975
23. Liepe, F.: "Stoffvereinigen in fluiden Phasen" in Verfahrenstechnishen Berechnungsunterlagen VCH Verlagsgesellschaft 1988
24. Möckel, H.-O.: Hydrodynamische Untersuchungen in Rührmaschinen. Dissertation Ingenieurhochschule Köthen 1978
25. Laufhütte, H.-D.: Turbulenzparameter in gerührten Fluiden. Dissertation TU München 1986
26. Geißler, R. K.: Fluiddynamik und Leistungseintrag in turbulent gerührten Suspensionen. Dissertation TU München 1991
27. Handa, A.: Ph.D. Thesis, University of Birmingham. 1986
28. Tramper, J., Vlak, J. M.: Preprints der GVC-Vortragstagung in Tübingen 1987, 189–201
29. Hülscher, M.: Fortschritt-Bericht Verfahrenstechnik. Reihe 3 (1990) 229 VDI-Verlag
30. Riquarts, H. P.: Chem.-Ing. Tech. 54 (1982) MS1023/82

Received June 11, 1992

H.-J. Henzler
D. J. Kauling
Zentrale Forschung/Bioverfahrenstechnik
BAYER AG
W-56 00 Wuppertal
Germany